ISSN (Print) 1226-1750
ISSN (Online) 2233-6656
Journal of Magnetics 17(4), 261-264 (2012) http://dx.doi.org/10.4283/JMAG.2012.17.4.261

Interfacial Properties in Cu-phthalocyanine-based Hybrid Inorganic/Organic Multilayers

Nyun Jong Lee[1], Eisuke Ito[2], Yu Jeong Bae[1], and Tae Hee Kim[1]*

[1]*Department of Physics, Ewha Womans University, Seoul 120-750, Korea*
[2]*Flucto-Order Functions Research Team, RIKEN Advanced Science Institute, Wako, Saitama 351-0198, Japan*

(Received 29 October 2012, Received in final form 13 December 2012, Accepted 13 December 2012)

Interfacial properties of 5 nm MgO(001)/7 nm Fe(001)/1.8 nm MgO(001)/t nm Cu-phthalocyanine (CuPc) hybrid multilayers with t = 0, 1, 7, and 10 were investigated by using x-ray photoemission spectroscopy (XPS). Rather sharp interfacial properties were observed in the CuPc films grown on an epitaxial MgO/Fe/MgO(001) trilayer than a MgO/Fe(001) bilayer. This work suggests a new way to improve device performance of organic spintronic devices by utilizing an artificially grown MgO(001) thin layer.

Keywords : inorganic/organic hybrid structure, interfacial properties, XPS, Cu-phthalocyanine film, organic spintronic devices

1. Introduction

For last decades, spintronics has been developed based on solid-state inorganic materials, and is now extended further to organic semiconductor (OSC) materials which offer many advantages such as light weight, mechanical flexibility, versatility, etc. Recent achievements in the field of organic spintronics open up pathways to a new generation of spintronic devices with higher integration density, lower power consumption and multifunctionality [1-4]. However, OSCs-based spintronic devices still possess some challenges and hindrances in device performance, indicating that major limiting factors of fundamental and technological nature remain to be understood and controlled.

The growth of organic films is one of those obstacles for the realization of spintronic devices, especially in order to obtain smooth films suitable for inorganic (I)/organic (O) hybrid multilayer structures that are important for their device applications, since the device performance is extremely sensitive to not only the materials but also the interfacial properties. Thus, different physical and chemical surface (interface) treatments have been widely utilized to control efficiently charge injection and transport in those devices [5, 6]. More interestingly, introducing an ultrathin oxide interface layer between a metal and an organic layer was suggested to improve the device efficiency [7-9]. Enhancement of room-temperature (RT) magnetoresistance in a Co/Alq_3/NiFe magnetic tunnel junction (MTJ) has been observed by inserting an Al_2O_3 layer less than 1 nm thick between Co and Alq_3 [10]. Lately, for an Fe(001)/Cu-phthalocyanine (CuPc)/Co MTJ, the improved device functionality and reliability were reported in our earlier study by introducing a thin epitaxial MgO(001) layer at the Fe(001)/CuPc interface [11]. Here, MgO(001) acts as a spin filter [12, 13] for electrons tunneling from the Fe electrode into the CuPc which is one of the π-conjugated oligomers used widely for organic thin film devices due to its high thermal and chemical stability. This led us to investigate the MgO(001)-based I/O hybrid structures for spintronic device applications working at RT.

This work was preliminary focused on the interfacial properties of the hybrid Fe(001)/MgO(001)/CuPc multilayers by using XPS which is a well-known versatile surface analysis technique used for compositional and chemical states analysis. It is expected that polarized charge (or electron) could be improved by inserting the thin MgO(001) interface layer, modifying the energy band structure at the Fe(001)/CuPc interface and preventing the Fe surface contamination due to air exposure during the sample transfer from ultra-high vacuum-molecular beam epitaxy (UHV-

*Corresponding author: Tel: +82-2-3277-4255
Fax: +82-2-3277-4255, e-mail: taehee@ewha.ac.kr

MBE) chamber to high vaccuum (HV)-thermal evaporation chamber. From this, the new approach to improve device performance by engineering the interfacial properties at nanoscale with the high-purity artificially grown oxide thin film is discussed.

2. Experiments

We used a UHV-MBE film evaporation system to stack successively inorganic elements beyond chemically etched p-type Si(001) wafers. The base pressure of the UHV-MBE was lower than ~1 × 10^{-10} Torr. The epitaxial 8 nm MgO(001)/15 nm Fe(001)/1.8 nm MgO(001) multilayers were formed at 250 °C with low deposition rate of 0.003 nm/s. During the deposition the pressure was kept lower than 3 × 10^{-9} Torr. CuPc films of thickness ranging from 1 to 10 nm were deposited at RT beyond Si(001)/8.0 nm MgO/15 nm Fe/1.8 nm MgO by HV-thermal evaporation (base pressure ~2 × 10^{-7} Torr): see a schematic in Fig. 2(f). It should be noted that air-exposure on the MgO top surface is inevitable during the sample transfer from the UHV-MBE chamber to the HV-thermal evaporator.

In order to investigate the thin CuPc film growth mode and characterize the interfacial properties of our samples, XPS spectra were obtained using a Theta Probe (Thermo Scientific) with monochromatic Al K_α x-ray source (1486.6 eV).

Additionally, the structural characteristics were performed by using X-ray powder diffraction technique (XRD) for the Si(001)/5 nm MgO/15 nm Fe/3.6 nm MgO/t nm CuPc (t = 0 and 10) hybrid multilayer.

3. Results and Discussion

The XRD pattern of the 10 nm thick CuPc film grown on the 5 nm MgO/15 nm Fe/3.6 nm MgO(001) trilayer is shown in Fig. 1. A strong diffraction peak, corresponding to the (002) lattice plane of β-phase CuPc, appears at 2θ = 7.15° which is quite close to the position expected from the reference data. The XRD pattern indicates that the Fe and MgO buffer layers are strongly (001) oriented, only

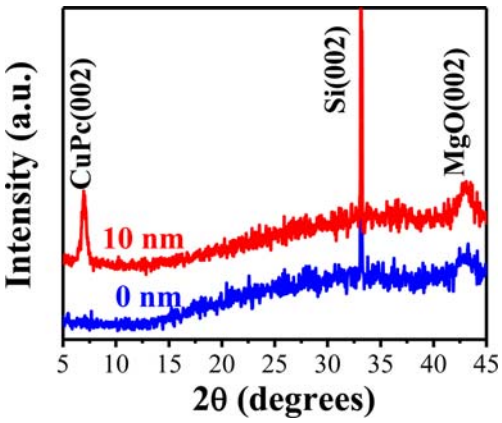

Fig. 1. (Color online) X-ray diffraction patterns of 8 nm MgO(001)/15 nm Fe(001)/1.8 nm MgO(001)/t nm CuPc (t = 0 and 10) multilayers grown on HF-etched Si(001) substrate.

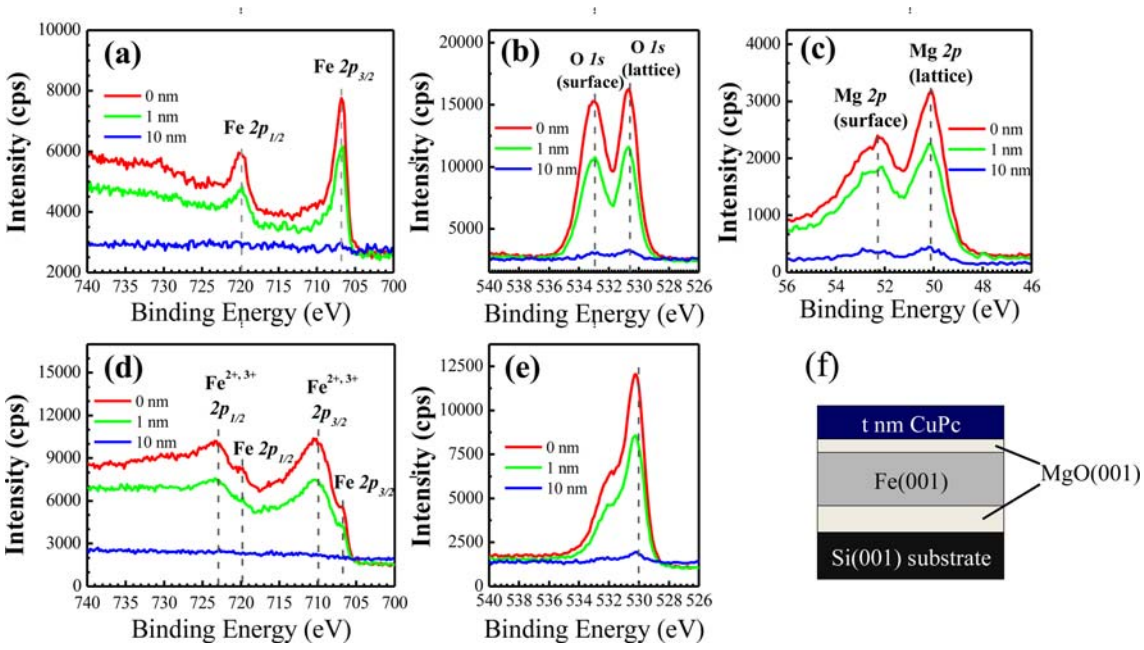

Fig. 2. (Color online) Evolution of Fe 2p (a), O 1s (b), and Mg 2p (c) for the CuPc films grown on Si(001)/MgO(001)/Fe(001)/MgO(001) as a function of t (t = 0, 1, 7, and 10); XPS spectra of Fe 2p (d), O 1s (e) for the CuPc films grown on Si(001)/MgO(001)/Fe(001) indicating the Fe oxidation state. Figure (f) shows a schematic of the film structure.

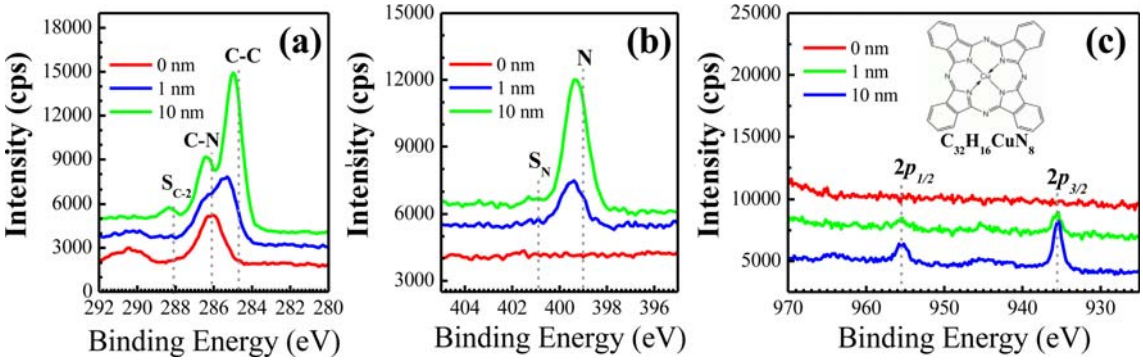

Fig. 3. (Color online) Evolution of C 1s (a), N 1s (b), and Cu 2p (c) as a function of t (t = 0, 1, and10) for the CuPc films grown on Si(001)/MgO(001)/Fe(001)/MgO(001).

the (002) diffraction peak of *fcc* MgO is shown. Consequently the CuPc films deposited on the epitaxial Fe/MgO(001) buffer layer are also predominantly (001) textured. The (001) orientation of the MgO/Fe/MgO trilayer was extremely dependent on the film growth conditions, especially the low deposition rate of 0.003 nm/s and ultra-high vacuum, the pressure lower than 3×10^{-9} Torr are required during the deposition.

To investigate the MgO(001)/CuPc and Fe(001)/CuPc interface, we performed a thickness dependent XPS study of CuPc films grown on both 8 nm MgO/15 nm Fe/1.8 nm MgO(001) and 8 nm MgO/15 nm Fe(001) buffer layer. The CuPc films with thickness of t (t = 0, 1, 7, and 10 nm) were grown at RT. The core-level photoemission spectra show no observable chemical shifts in Fe 2p and O 1s peaks in Fig. 2(a) and (b), respectively. The standard peak positions of Fe $2p_{3/2}$ and Fe $2p_{1/2}$ for the Fe, Fe^{2+}, and Fe^{3+} are found in the literature and marked with dashed line in Fig. 2(a) and (c) [14-16]. These spectra for t = 0-7 nm show almost identical shape indicating the same origin: the Fe and MgO surface. Since, for electron that are normally used in XPS, the attenuation lengths are about 1-10 monolayers, all peak intensities of Fe and MgO decreased gradually with increase in t. Finally for t = 10 nm, these signals become totally buried under the CuPc layer.

The XPS spectrum of a MgO film (1.8 nm) in Fig. 2(b) shows the presence of two oxygen peaks in the O 1s core level, similar to that reported in Ref. [16]. The lower binding energy (LBE) peak was attributed to the lattice oxygen in the MgO. The higher binding energy (HBE) peak can be seen in both the O 1s spectrum in Fig. 2(b) and in the Mg 2p spectrum in Fig. 2(c). The higher binding energies are surface localized. Exposure to ambient conditions during the sample transfer for a minute caused the HBE peaks to be enhanced, which suggests that they are both related to the formations of the surface hydroxide species [17]. Casey *et al.* reported the possibility to use the ratio of two oxygen peaks as a measure of film surface area and the flatness of the film [17]. It is noticeable that O 1s HBE peak intensity was reduced in Fig. 2(e) when the CuPc films were grown directly on the Fe(001) layer. Two O 1s peak positions shifted to lower (~1 eV) in comparison with those in Fig. 2(b). It has been also shown in previous studies that the peak positions of Fe $2p_{3/2}$ and Fe $2p_{1/2}$ depend on the ionic states of Fe [14, 16]. All these results indicate that for the sample without the MgO(001) layer between Fe and CuPc, the oxidation of Fe surface occurred due to exposure to the air during sample transfer.

Fig. 3 shows the XPS spectra of C 1s, N 1s, Cu $2p_{3/2}$ and Cu $2p_{1/2}$ with different thickness of CuPc deposited on MgO(001). It is remarkable that, for the C 1s, N 1s peaks, the peak positions shifted as a function of CuPc thickness while no peak shift was observed for Cu $2p_{3/2}$ and Cu $2p_{1/2}$. Particularly, the spectrum of C 1s consisted of three different features (C-C, C-N, and S_{C-2}) was observed due to the different chemical environment: one is the C-C bond resulted from the aromatic carbon atoms which interact with hydrogen (H) or the other carbon (C) atoms. The other is the C-N bond resulted from pyrrole carbon linked to nitrogen (N). Additionally, π-π^* satellite (S_{C-2}) feature is favourable for the description of CuPc. Satellites of conjugated carbon compounds are caused by energy loss of the photoelectrons due to simultaneously excited $\pi \rightarrow \pi^*$ transitions [18]. For the thinner CuPc thickness of 1 nm, larger peak shift of C 1s and N 1s was observed than the thicker film (10 nm). These binding energy shifts could be attributed to the strong interaction of C and N atoms with O of the MgO underlayer.

4. Summary

In order to improve the CuPc film structure for organic

thin film device applications, a new approach was suggested by inserting an ultra-thin MgO(001) epitaxial layer in the I/O hybrid structures. The systematic XPS surface (interface) analysis was carried out as a function of thickness for the CuPc films grown on both epitaxial MgO/Fe/MgO(001) trilayer and a MgO/Fe(001) bilayer beyond HF-etched Si(001) substrates. We confirmed that the MgO(001) layer well-known as a spin filter could protect the Fe(001) layer against oxidation when the surface is exposed to air. Moreover, beyond the MgO(001) layer, highly textured (001) CuPc film growth with smooth surface morphology was observed by structural analysis. However, further investigations are required for the realization of fully epitaxial I/O hybrid multilayer structures.

Acknowledgement

This work is supported by NRF grants (no. 2008-0062239, 2010-0006749, and 2011-0017209).

References

[1] K. Al-Sharmery, H.-G. Rubahn, and H. Sitter, Organic Nanostructures for Next Generation Devices, Springer, Berlin (2008) pp. 263-345.
[2] F. Sawano, I. Terasaki, H. Mori, T. Mori, M. Watanabe, N. Ikeda, Y. Nogami, and Y. Noda, Nature **437**, 522 (2005).
[3] Y.-S. Lai, C.-H. Tu, D.-L. Kwong, and J. S. Chen, Appl. Phys. Lett. **87**, 122101 (2005).
[4] V. A. Dediu, L. E. Hueso, I. Bergenti, and C. Taliani, Nature Mater. **8**, 707 (2009).
[5] Z. H Xiong, D. Wu, Z. V. Vardeny, and J. Shi, Nature **427**, 821 (2004).
[6] J.-W. Yoo, C.-Y. Chen, H. W. Jang, C. W. Bark, V. N. Prigodin, C. B. Eom, and A. J. Epstein, Nature Mater. **9**, 638 (2010).
[7] W. J. M. Naber, S. Faez, and W. G. van der Wiel, J. Phys. D **40**, R205 (2007).
[8] Y. Q. Zhan, X. J. Liu, E. Carlegrim, F. H. Li, I. Bergenti, P. Graziosi, V. Dediu, and M. Fahlman, Appl. Phys. Lett. **94**, 053301 (2009).
[9] H. W. Choi, S. Y. Kim, W.-K. Kim, K. Hong, and J.-L. Lee, J. Appl. Phys. **100**, 064106 (2006).
[10] T. S. Santos, J. S. Lee, P. Migdal, I. C. Lekshmi, B. Satpati, and J. S. Moodera, Phys. Rev. Lett. **98**, 016601 (2007).
[11] Y. J. Bae, N. J. Lee, T. H. Kim, H. Cho, C. Lee, L. Fleet, and A. Hirohata, Nanoscale Research Letters **7**, 650 (2012).
[12] S. Yuasa, T. Nagahama, A. Fukushima, Y. Suzuki, and K. Ando, Nature Mater. **3**, 868 (2004)
[13] W. H. Butler, X.-G. Zhang, T. C. Schulthess, and J. M. Maclaren, Phys. Rev. B **63**, 054416 (2001).
[14] S. J. Roosendaal, B. van Asselen, J. W. Elsenaar, A. M. Vredenberg, and F. H. P. M. Habraken, Surf. Sci. **442**, 329 (1999).
[15] T. Yamashita and P. Hayes, J. Electron Spectrosc. Relat. Phenom. **152**, 6 (2006).
[16] C. Ruby, B. Humbert, and J. Fusy, Surf. Interface Anal. **29**, 377 (2000).
[17] P. Casey, G. Hughes, E. O'Connor, R. D. Long, and P. K. Hurley, J. Phys.: Conference Series **100**, 042046 (2008).
[18] G. Beamson and D. Briggs, High Resolution XPS of Organic Polymers, John Wiley & Sons, Chichester (1992).